ARTICLE

Journal of Materials Chemistry
www.rsc.org/materials

Synthesis and properties of highly sulfonated proton conducting polyimides from bis(3-sulfopropoxy)benzidine diamines†

Yan Yin, Jianhua Fang, Tatsuya Watari, Kazuhiro Tanaka, Hidetoshi Kita and Ken-ichi Okamoto*

Department of Advanced Materials Science & Engineering, Faculty of Engineering, Yamaguchi University, 2-16-1 Tokiwadai, Ube, Yamaguchi, 755-8611, Japan. E-mail: okamotok@yamaguchi-u.ac.jp; Fax: +81-836-85-9601; Tel: +81-836-85-9660

Received 21st October 2003, Accepted 23rd December 2003
First published as an Advance Article on the web 19th February 2004

Two novel sulfonated diamine isomers, 2,2′-bis(3-sulfopropoxy)benzidine (2,2′-BSPB) and 3,3′-bis(3-sulfopropoxy)benzidine (3,3′-BSPB), were successfully synthesized and the highly sulfonated polyimides (SPIs) with sulfonic acid groups in the side chains were prepared from 1,4,5,8-naphthalenetetracarboxylic dianhydride (NTDA) and BSPB monomers. Transmission electron microscopy (TEM) analysis revealed that these side-chain-type SPI membranes have a microphase-separated structure composed of hydrophilic side chain domains and hydrophobic polyimide main chain domains. They showed high proton conductivities similar to or higher than those of Nafion 117 in the high relative humidity range (>70% RH). The proton conducting behavior was analyzed by percolation theory. Despite their high ion exchange capacity (IEC = 2.89 meq. g^{-1}) and high water uptakes, they displayed much better water stability than common sulfonated polyimides with the sulfonic acid groups directly bonded to the polymer backbone. This is probably due to the microphase-separated structure of the membrane and the strong basicity of BSPB diamine moieties resulting from the electron donating effect of the propoxy groups. The sulfopropoxy groups were stable against aging in acidic aqueous solution at 373 K. Both the polyimide membranes showed good mechanical strength under high moisture conditions (about 6 GPa at 90% RH) and displayed anisotropic membrane swelling.

Introduction

Fuel cells are electrochemical energy converters, transforming chemical energy directly into electricity. During the past decades, great effort has gone into the development of polymer electrolyte fuel cells (PEFC) for both mobile and stationary applications.[1,2] Nafion (Du Pont), a perfluorosulfonic acid membrane, and other related perfluoropolymer membranes have been utilized as excellent proton exchange membranes for PEFC for a long time. However, some disadvantages such as high cost, low operation temperature, and high methanol permeability limit their industrial application. Therefore, a major research goal would be to identify and achieve novel, high performance and low cost proton conductive materials. So far, two types of sulfonated polymers depending on the position of sulfonic acid groups have been studied. Those with sulfonic acid groups directly bonded to the polymer backbone are noted as main-chain-types; others with sulfonic acid groups attached to the side chains are distinguished as side-chain-types. Up to now, main-chain-type sulfonated polymers such as sulfonated polysulfones,[3] sulfonated polyether ether ketones,[4] sulfonated polyphosphazenes,[5] and sulfonated polyimides[6–14] have been widely developed as possible substitutes of perfluorinated ionomers. The major problem associated with most of these polymer membranes is that their water stability is rather poor (highly swollen or even dissolved in water) when their ion exchange capacities (IECs) reach a high level (> ~2.0 meq g^{-1}). Our group has synthesized a series of main-chain-type sulfonated polyimides (SPIs) from novel sulfonated diamines, among which SPIs derived from 4,4′-bis(4-aminophenoxy)biphenyl-3,3′-disulfonic acid (BAPBDS) displayed much better membrane performance than other SPIs from the view points of proton conductivity, water stability and membrane swelling.[14]

Side-chain-type sulfonated polymers have also been studied by several research groups. Gieselman and Reynolds[15,16] prepared a series of polybenzimidazole (PBI) and poly(*p*-phenyleneterephthalamido) (PPTA)-based polyelectrolytes with propane or methylbenzene sulfonic acid groups but the proton conductivity was not mentioned. The processability was improved after the introduction of the pendent groups but the water stability was poor. For example, PPTA-PS (propanesultone) became water soluble with a 50% substitution, and PBI-PS was soluble in water with 60% substitution. Bae *et al.*[17] synthesized a series of sulfoalkylated PBI as polymer electrolytes from alkylsultone and PBI. Rikukawa *et al.*[18] reported that PBI-BS (butanesultone) displayed high proton conductivities in the range of 0.07 to 0.3 S cm^{-1} at 90% RH and in the temperature range of 303 to 353 K. They also reported on proton conductivities lower than 10^{-2} S cm^{-1} for the same kind of membrane by impedance spectroscopy using a single fuel cell, which was operated under the conditions of 100% RH and 333–373 K.[17] Roziere and co-workers[19] reported on the proton conductivities in the order of 10^{-2} S cm^{-1} (at 313 K and 100% RH) of methylbenzenesulfonated PBI at a high sulfonation degree (75%) prepared by grafting of sulfonated aryl groups on to PBI. Hay *et al.*[20,21] synthesized a series of sulfonated arylene ether/fluorinated alkane copolymers, and reported on a proton conductivity of 3.4×10^{-3} S cm^{-1} which was stable up to 443 K. Their membranes showed relatively good water stability (could keep film form after soaked in water at 373 K for more than one week). Rikukawa and co-workers[22,23] synthesized a series of sulfonated poly(4-phenoxybenzoyl-1,4-phenylene) (S-PPBP) and reported on a proton conductiviy in the order of 10^{-2} S cm^{-1} at room temperature and 100% RH for the membrane with a high sulfonation degree (65%).

† Electronic supplementary information (ESI) available: ^{1}H NMR spectra of BSPB diamines and IR spectra of resulting polyimide membranes. See http://www.rsc.org/suppdata/jm/b3/b313276e/

DOI: 10.1039/b313276e

The water stability of the above mentioned polymer membranes is not very good. Generally, side-chain-type polymers are expected to form microphase-separated structures relatively easily which is favorable for proton transport. If the polymers have strong interchain interactions that allow the dense packing of polymer chains, the water stability might be greatly improved. Aromatic polyimides are known to have excellent thermal stability, high mechanical strength and modulus.[24] They also have good film forming ability and superior solvent-resistance because of the strong charge transfer interaction between polymer chains. These merits of polyimides are just what are required for polymer electrolyte membranes. In a previous paper,[25] a novel side-chain-type polyimide has been prepared from a propoxy sulfonated diamine monomer, 3-(2′,4′-diaminophenoxy)propane sulfonic acid (DAPPS), and the similar proton conductivity as well as better water stability was found compared with some main-chain-type SPIs with the similar IEC.

However, the DAPPS-based polyimide had a relatively low IEC resulting in a low proton conductivity, and the meta-oriented diamine moieties led to good solubility properties and thus relatively low membrane durability towards water. In this paper, two novel sulfopropoxylated diamine isomers, 2,2′-bis(3-sulfopropoxy)benzidine (2,2′-BSPB) and 3,3′-bis(3-sulfopropoxy)benzidine (3,3′-BSPB), were synthesized and the corresponding side-chain-type SPIs with higher IEC were prepared. Their physical properties, membrane morphology, proton conductivity, and water stability were investigated.

Experimental

1,4,5,8-Naphthalenetetracarboxylic dianhydride (NTDA), 2-nitrophenol, 3-nitrophenol and 3-bromopropane sulfonic acid sodium salt were purchased from Tokyo Kasei Co., and NTDA was purified by vacuum sublimation prior to use. Dimethylformamide (DMF), dimethyl sulfoxide (DMSO) and triethylamine (Et_3N) were purchased from Wako Chemical Co. and were purified by distillation under reduced pressure and dehydrated with 4 Å molecular sieves prior to use. Other reagents were used as received. Ultra-pure water was obtained from a Millipore Milli-Q purification system.

Synthesis of 3-(3′-nitrophenoxy)propane sulfonic acid sodium salt (NPPS, 2)

13.9 g (100 mmol) of 3-nitrophenol and 120 ml of DMF were added to a completely dried 300 ml 4-neck of flask equipped with a Dean–Stark trap, with stirring under a nitrogen flow. K_2CO_3 (20.7 g, 150 mmol) and 20 ml of toluene were added successively. The reaction mixture was stirred at room temperature for 30 min and then heated to reflux for two hours. After cooling to room temperature, 22.5 g (100 mmol) of 3-bromopropanesulfonic acid sodium salt was fed to the flask in one portion. The reaction mixture was reheated up to 383 K for 24 h. After cooling to room temperature, the resulting reaction mixture was poured into acetone, the solid was filtered and thoroughly washed with acetone and then dried *in vacuo* at 333 K for 10 h. The obtained solid was dissolved in 100 ml of DMSO and the mixture was stirred at room temperature for 30 min. The insoluble inorganic salt was filtered off, and the filtrate was distilled under reduced pressure to remove the solvent (DMSO). The residue was washed with acetone, and then dried *in vacuo* at 333 K for 20 h. The crude product was purified by recrystallization from methanol to give 25 g of compound **2**. Yield: 86%; mp (DSC): 503 K; IR (KBr, cm^{-1}): 3397, 1579, 1526, 1408, 1357, 1321, 1248, 1186, 1161, 1050, 1017, 877, 797, 736, 594. ^{1}H NMR (ppm, DMSO-d_6): 7.87–7.76 (d, 1H, phenyl ring), 7.70–7.65 (s, 1 H, phenyl ring), 7.62–7.50 (t, 1 H, phenyl ring), 7.48–7.34 (m, 1 H, phenyl ring), 4.28–4.12 (t, 2 H, $-OCH_2-$), 2.66–2.54 (t, 2 H, $-CH_2SO_3Na$), 2.14–1.94 (m, 2 H, $-CH_2-$).

Synthesis of 3,3′-bis(3-sulfopropoxy)azobenzene disodium salt (BSPAB, 3)

To a completely dried 100 ml 4-neck flask were charged 5.66 g (20.0 mmol) of compound **2**, 15 ml of water together with 15 ml of methanol, and 4.6 g (70.8 mmol) of zinc powder under a nitrogen flow. The mixture was stirred and heated to 363 K, then 5 g (62.5 mmol) of NaOH in 10 ml of H_2O was added dropwise. After the NaOH solution was completely added, the reaction mixture was further stirred at 363 K for 4 h. After cooling to room temperature, the reaction mixture was filtered, and the filtrate was distilled under reduced pressure. The obtained solid was washed with ethanol, and dried *in vacuo* at 333K for 20 h to give 4.4 g of orange compound **3**. Yield: 88%; mp (DSC): 549 K; IR (KBr cm^{-1}): 2934, 1601, 1475, 1330, 1199, 1138, 1059, 996, 862, 795, 737, 690. ^{1}H NMR (ppm, DMSO-d_6): 7.59–7.45 (m, 4 H, phenyl ring, overlapped), 7.43–7.38 (s, 2 H, phenyl ring), 7.20–7.10 (m, 2 H, phenyl ring), 4.21–4.12 (t, 4 H, $-OCH_2-$), 2.68–2.53 (t, 4 H, $-CH_2SO_3Na$), 2.13–1.98 (m, 4 H, $-CH_2-$).

Synthesis of 3,3′-bis(3-sulfopropoxy)hydrazobenzene disodium salt (BSPHB, 4)

To a completely dried 100 ml 4-neck flask were fed 4.53 g (9.0 mmol) of compound **3**, 45 ml of water and 4.5 ml of acetic acid, stirred under a nitrogen flow. When the mixture was heated to 363 K, 4.5 g of zinc powder was added quickly. The mixture was further stirred for one hour. After cooling to room temperature, the reaction mixture was filtered, and the filtrate was distilled under reduced pressure. The obtained solid was thoroughly washed with ethanol and dried *in vacuo* to give 3.96 g of grey solid of compound **4**. Yield: 87%; mp (DSC): 577 K; IR (KBr cm^{-1}): 3435, 2952, 2643, 1609, 1540, 1498, 1469, 1445, 1406, 1278, 1181, 1043, 964, 856, 780, 734, 596. ^{1}H NMR (ppm, DMSO-d_6): 7.28–7.10 (t, 2 H, phenyl ring), 6.70–6.50 (m, 6 H, phenyl ring, overlapped), 4.12–3.92 (t, 4 H, $-OCH_2-$), 2.65–2.52 (t, 4 H, $-CH_2SO_3Na$), 2.10–1.94 (m, 4 H, $-CH_2-$).

Synthesis of 2,2′-bis(3-sulfopropoxy)benzidine (2,2′-BSPB, 5)

To a completely dried 100 ml 4-neck flask were added 2.0 g of compound **4**, 10 ml of water and 10 ml of concentrated hydrochloric acid, stirred under a nitrogen flow. The mixture was heated to 373 K for 2 h and then cooled to room temperature. The resulting precipitate was filtered off and dried *in vacuo* to give 1.2 g of grey white compound **5**. Yield: 60%; mp (DSC): 614 K; IR (KBr cm^{-1}): 3435, 2926, 2633, 2070, 1604, 1579, 1519, 1494, 1433, 1391, 1315, 1181, 1043, 979, 795, 744. ^{1}H NMR (ppm, DMSO-d_6): 6.82–6.70 (d, 1 H, phenyl ring), 6.24–6.18 (s, 1 H, phenyl ring), 6.17–6.04 (d, 1 H, phenyl ring), 5.13–4.68 (s, 2 H, amino group), 3.93–3.79 (t, 2 H, $-OCH_2-$), 1.96–1.78 (m, 2 H, $-CH_2-$).

Synthesis of 3,3′-bis(3-sulfopropoxy)benzidine (3,3′-BSPB)

The synthesis of 3,3′-BSPB was analogous to that of 2,2′-BSPB using 2-nitrophenol and 3-bromopropane sulfonic acid sodium salt as the starting materials. The overall yield was about 30%. ^{1}H NMR (ppm, DMSO-d_6): 7.02–6.92 (s, 1 H, phenyl ring), 6.92–6.82 (d, 1 H, phenyl ring), 6.73–6.59 (d, 1 H, phenyl ring), 4.95–4.45 (s, 2 H, amino group), 4.19–4.02 (t, 2 H, $-OCH_2-$), 2.18–1.98 (m, 2 H, $-CH_2-$).

Synthesis of NTDA-BSPB polyimides

To a 100 ml completely dried 4-neck flask were added 1.84 g (4 mmol) of 2,2′-BSPB (or 3,3′-BSPB), 14 ml of *m*-cresol, and 2 ml of triethylamine, with stirring under a nitrogen flow. After

the 2,2′-BSPB was dissolved completely, 1.072 g (4 mmol) of NTDA and 0.68 g of benzoic acid were charged to the flask. The mixture was heated to 353 K for 4 h and 453 K for 20 h, respectively. After cooling to room temperature, an additional 40 ml of *m*-cresol was added and the mixture was reheated to 353 K to dilute the highly viscous solution. Then the reaction mixture was poured into acetone, the resulting fiber-like precipitate was collected by filtration, and dried *in vacuo* at 333 K for 20 h. IR spectra of NTDA-BSPB polyimide films (proton form) are given in the ESI†. NTDA-2,2′-BSPB (cm^{-1}): 3432, 2965, 1712, 1672, 1580, 1493, 1449, 1420, 1350, 1253, 1201, 1121, 1095, 1035, 984, 874, 819, 798, 774, 743, 630. NTDA-3,3′-BSPB (cm^{-1}): 3429, 2964, 1713, 1671, 1604, 1581, 1500, 1449, 1414, 1351, 1258, 1200, 1156, 1100, 1036, 984, 865, 799, 769, 757, 711, 627.

Membrane formation and proton exchange

The resulting polyimides (in triethylammonium salt form) were dissolved in *m*-cresol, and the membranes were obtained by solution casting at 383 K for 10 h. The as-cast films were soaked in methanol at 333 K for 1 h to remove the residue solvent, and then the proton exchange treatment was performed by immersing the films into 1.0 M hydrochloric acid solution at room temperature for 24 h. The proton-exchanged films were thoroughly washed with water and then dried *in vacuo* at 423 K for 10 h.

Measurements

Infrared (IR) spectra were recorded on a FT/IR-610 (JASCO, Japan) spectrometer for monomer powder as KBr pellets or polymer thin film. Differential scanning calorimetry (DSC) was performed with a RIGAKU DSC-5200 at a heating rate of 5 K min^{-1}. ^1H NMR spectra were recorded on a JEOL EX270 (270 MHz) instrument. Thermogravimetry-mass spectroscopy (TG-MS) was measured with a MS (SHIMADZU)-TG (RIGAKU)/8120 in helium (flow rate: 100 cm^3 min^{-1}) at a heating rate of 5 K min^{-1}. Dynamic mechanical spectra were measured on a DVA-220/L2 spectrometer at temperatures ranging from room temperature to 373 K and RHs ranging from 0% to 90%. Transmission electron microscopy (TEM) analysis for SPI membrane was performed in UBE Scientific Analysis Laboratory, Japan. The membrane sample in proton form was brought into the $-SO_3Ag$ form by immersing it in 0.5 M $AgNO_3$ solution overnight in order to stain the ionic domains and then thoroughly rinsed with water, dried at room temperature for 24 h before measurement.

Proton conductivity was measured using an electrochemical impedance spectroscopy technique over the frequency range from 100 Hz to 100 KHz (Hioki 3552). A four-point-probe cell with two pairs of blackened platinum plate electrodes pressed with a sample membrane was mounted in a sealed Teflon cell case. The cell was placed in either a thermo-controlled humidic chamber or water to measure the humidity and temperature dependence of proton conductivity. The resistance value associated with the membrane conductance was determined from high-frequency intercept of the impedance with the real axis. Proton conductivity (σ) was calculated from eqn. (1):

$$\sigma = d/(t_s\, w_s\, R) \tag{1}$$

where d is the distance between the two electrodes, t_s and w_s are the thickness and width of the membrane equilibrated at 70% RH (as a standard condition), respectively, and R is the resistance value measured. For the measurement in liquid water, as the dimensional change could not be neglected, the measured or corrected membrane thickness was used in the calculation of σ.

Water vapor sorption experiments were conducted at different water activities ($a_w < 1$) at 323 K using a sorption apparatus (BEL-18SP) by means of a volumetric method. The weight of membrane samples used was 100 mg. Water uptake in liquid water was also measured by immersing two sheets of films (20–30 mg per sheet) of polyimide into water at a given temperature for 3–5 h. Then the films were taken out, wiped with tissue paper, and quickly weighed on a microbalance. Water uptake (WU) of the films was calculated from eqn. (2):

$$WU = (W_S - W_d)/W_d \times 100 \tag{2}$$

where W_d and W_s are the weights of dry and corresponding water-swollen film sheets, respectively. Water uptake of the polyimide membrane was estimated from the average value of WU of each sheet.

The ion exchange capacity (IEC) was measured by classical titration. The membranes were soaked in a saturated NaCl solution. Released protons were titrated using 0.01 M NaOH solution. Density of SPI membranes (30 μm in thickness and 2.6 cm in diameter) equilibrated under a standard condition of 70% RH and in water was measured by floating method using mixtures of carbon tetrachloride and xylene at a room temperature. Dimensional change of the SPI membranes was investigated by immersing the round shape samples into water at room temperature for a given time, the changes of thickness and diameter were calculated from eqn. (3):

$$\begin{aligned} \Delta l_c &= (l - l_s)/l_s \\ \Delta t_c &= (t - t_s)/t_s \end{aligned} \tag{3}$$

where t_s and l_s are the thickness and diameter of the membrane equilibrated at 70% RH, respectively; t and l refer to those of the membrane immersed in liquid water for 5 h. In this case, the dry films were difficult to be measured due to the shrink after being dried at 423 K for 10 h. The shrinked films were first immersed in water to get smooth samples and then taken out and placed at ambient condition (70% RH) for 24 h, followed by the measurement of density and size as standards.

Results and discussion

Synthesis and characterization of monomers and polyimides

BSPB monomers were prepared by an analogous method and the synthetic routes are shown in Scheme 1. First, NPPS **2** was synthesized from compound **1** and 3-bromopropanesulfonic acid sodium salt. The azo compounds **3** were prepared from the reduction of **2** with zinc powder under basic conditions. The further reduction of **3** in the presence of weak acid gave the hydrazo compounds **4**. The diamine monomers **5** were obtained by rearrangement reactions of **4** in hydrochloric acid. ^1H NMR spectra of BSPB isomers in the presence of Et_3N are given in the ESI.† Et_3N was employed to liberate the amine groups and improve the solubility of BSPB monomers in DMSO-d_6. The ^1HNMR spectra are just consistent with the proposed structures of BSPB. Elementary analysis data of BSPB diamine isomers are listed in Table 1.

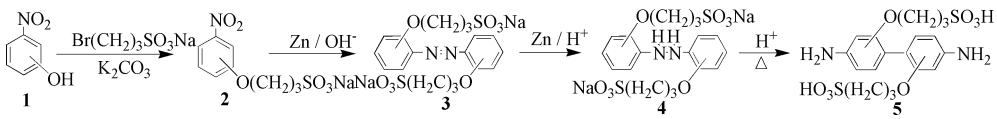

Scheme 1

Table 1 Elementary analysis of BSPB diamines and NTDA-2,2′-BSPB polyimide

		C (%)	H (%)	N (%)	O (%)	N/C
2,2′-BSPB	Found	46.32	5.17	6.02	28.22	0.1299
	Calcd.	46.94	5.25	6.08	27.79	0.1295
3,3′-BSPB	Found	46.72	5.29	6.09	27.87	0.1303
	Calcd.	46.94	5.25	6.08	27.79	0.1295
NTDA-2,2′-BSPB	Found	50.52	4.07	3.75	34.13	0.07422
	Calcd.	55.49	3.49	4.04	27.72	0.07281
	Calcd.[a]	51.06	4.10	3.72	32.61	0.07286

[a] Calculated values containing 8 wt% water.

The preparation of the polyimides, NTDA-2,2′-BSPB and NTDA-3,3′-BSPB was carried out according to a one-step polymerization method using *m*-cresol as the solvent in the presence of Et_3N and benzoic acid (as shown in Scheme 2). In this case Et_3N was employed to improve the solubility of BSPB by liberating the protonated amino groups and benzoic acid was used as a catalyst. The obtained polyimide membranes in triethylammonium salt form were proton-exchanged with 1.0 M HCl at room temperature for 20 h. The IEC values obtained from titration (2.72–2.80 meq g^{-1}) were slightly smaller than the theoretical value (2.89 meq g^{-1}). FT-IR spectra of the NTDA-BSPB thin films are given in the ESI. The peaks around 1712 cm^{-1} ($\nu_{sym}C{=}O$), 1672 cm^{-1} ($\nu_{asym}C{=}O$) and 1350 cm^{-1} (ν_{CN} imide) are attributed to the naphthalenic imido rings. The bands around 1201 cm^{-1} and 1035 cm^{-1} are assigned to the stretch vibration of sulfonic acid groups. The peak at about 1250 cm^{-1} is attributed to the vibration of the ether bond between the phenyl ring and propyl group and the peak at around 2965 cm^{-1} is assigned to the vibration of methyl groups on the side chain. The elementary analysis of NTDA-2,2′-BSPB is shown in Table 1. The slight difference between the calculated and found values came from the small amount of sorbed water in the SPI (about 8 wt%) due to the high IEC. Although, we could not determine the molecular weights of the polyimides by GPC or by light scattering because of the insolubility of the polyimides in tetrahydrafuran (THF) or 1-methylpyrrolidone (NMP), the facts that fiber-like precipitates were obtained when the polymer solutions were poured into acetone and very tough films were formed by solution cast suggest that high molecular weight polyimides were obtained.

TEM analysis was performed on Ag^+-stained SPI membranes because Ag^+ gives a good contrast. The cross section micrograph of NTDA-2,2′-BSPB membrane is shown in Fig. 1. The darker regions represent localized hydrophilic ionic domains and the lighter parts refer to hydrophobic polyimide backbone. The ionic domains with an average size of about 5 nm connected to each other to form proton conducting paths. This TEM image provides a direct evidence of a biphasic-morphology for this side-chain-type SPI. The microphase-separated structure imparts the superior mechanical strength, high proton conductivity and excellent water stability of the side-chain-type SPI membranes, which will be discussed later.

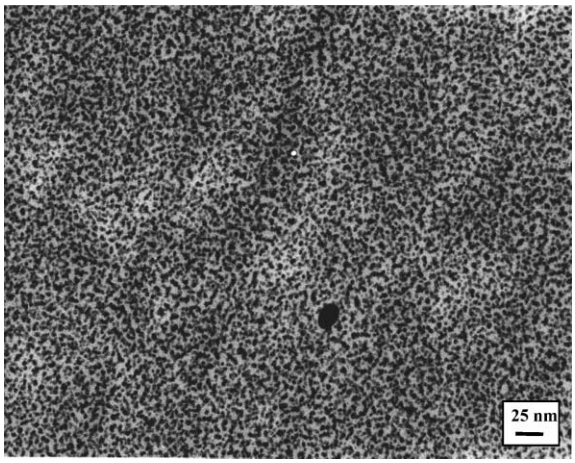

Fig. 1 TEM image of NTDA-2,2′-BSPB membrane (in Ag^+ salt form, cross section).

Thermal and mechanical analysis

Fig. 2 shows the thermal stability of NTDA-2,2′-BSPB polyimide membrane investigated by TG-MS. The initial weight loss around 373 K is ascribed to the loss of sorbed water in the sample. The second weight loss starting around 513 K is attributed to the decomposition of propoxy groups ($-OCH_2CH_2CH_2-$) and sulfonic acid groups judging from the evolution of propene (M = 42), propadine (M = 40), sulfur dioxide and water. The decomposition temperature of sulfonic acid groups is similar to or slightly lower than that of

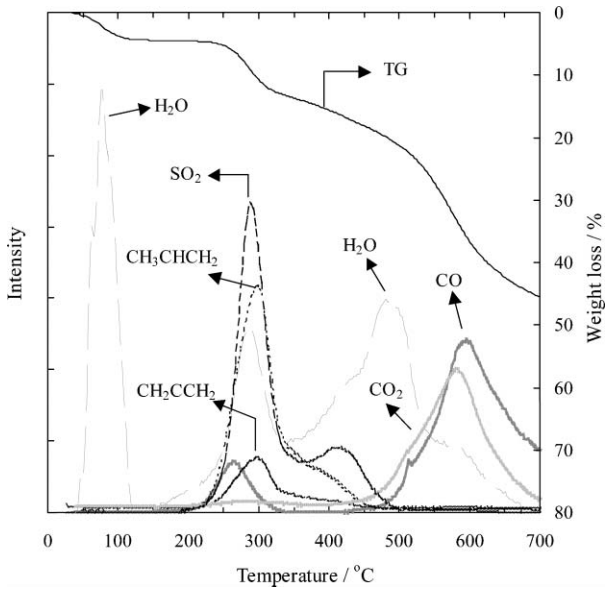

Fig. 2 Thermogravimetry-mass spectroscopy (TG-MS) of NTDA-2,2′-BSPB polyimide membrane.

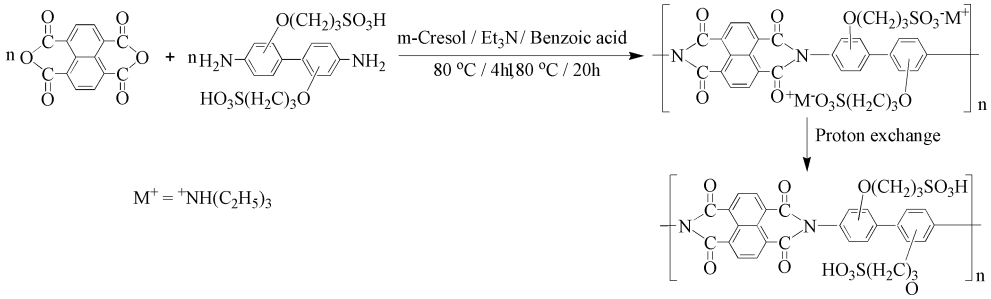

Scheme 2

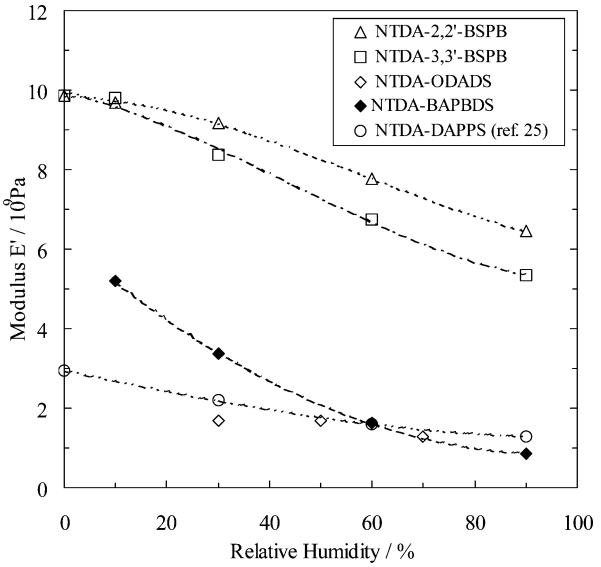

Fig. 3 Mechanical strength of SPI membranes as a function of relative humidity.

other wholly aromatic sulfonated polyimides.[6,12] A maximum evolution of sulfur dioxide was found at about 563 K. The third stage weight loss (723–973 K) is due to the decomposition of polymer main chain.

The dynamic moduli E's of SPI membranes under different moisture conditions are shown in Fig. 3. There was no significant change in E' as temperature increased from room temperature to 373 K. However, the E' is clearly dependent on the RH. At 10% RH, the E' was 9.6 GPa for NTDA-2,2′-BSPB and NTDA-3,3′-BSPB membranes. This was quite similar to that of the dry membranes (9.8 GPa). With a further increase in RH, the E' decreased gradually. This is because at a higher RH the membrane had a larger water uptake resulting in easier polymer chain relaxation and leading to larger membrane swelling. At 90% RH, the E' of NTDA-2,2′-BSPB membrane reduced to two thirds of the value of the dry state, whereas the E' of NTDA-3,3′-BSPB membrane decreased by about a half. It should be mentioned that these membranes held higher mechanical strength than the main-chain-type SPIs such as NTDA-ODADS and NTDA-BAPBDS and another side-chain-type SPI, NTDA-DAPPS, under high moisture conditions, probably due to the difference of membrane morphology.

Water vapor sorption

The water vapor sorption isotherms of SPIs and Nafion 117 are shown in Fig. 4. With an increase in water vapor activity (a_w), the water vapor sorption increased sigmoidally. NTDA-2,2′-BSPB and NTDA-3,3′-BSPB membranes showed similar water vapor sorption behavior in the whole range of a_w. Their water vapor uptakes were larger than those of Nafion 117 (Fig. 4a). The sorption isotherms in a form of the number of sorbed water molecules per sulfonic acid group, λ *vs.* a_w are shown in Fig. 4b. It is interesting that the λ-a_w isotherm of the main-chain-type SPI such as NTDA-BAPBDS,[14] was similar or close to that of Nafion 117 rather than those of the side-chain-type SPIs. The λ-a_w isotherms of NTDA-BSPB polyimide membranes were different from those of the former in the following two points. First, they showed much lower λ values in the range of $a_w < 0.5$. This means apparently much lower capacities of Langmuir sorption sites based on sulfonic acid groups for the side-chain-type SPIs. Second, their λ values increased significantly with an increase in a_w in the range of $a_w > 0.8$, probably due to larger molecular relaxation of polymer chains.[26]

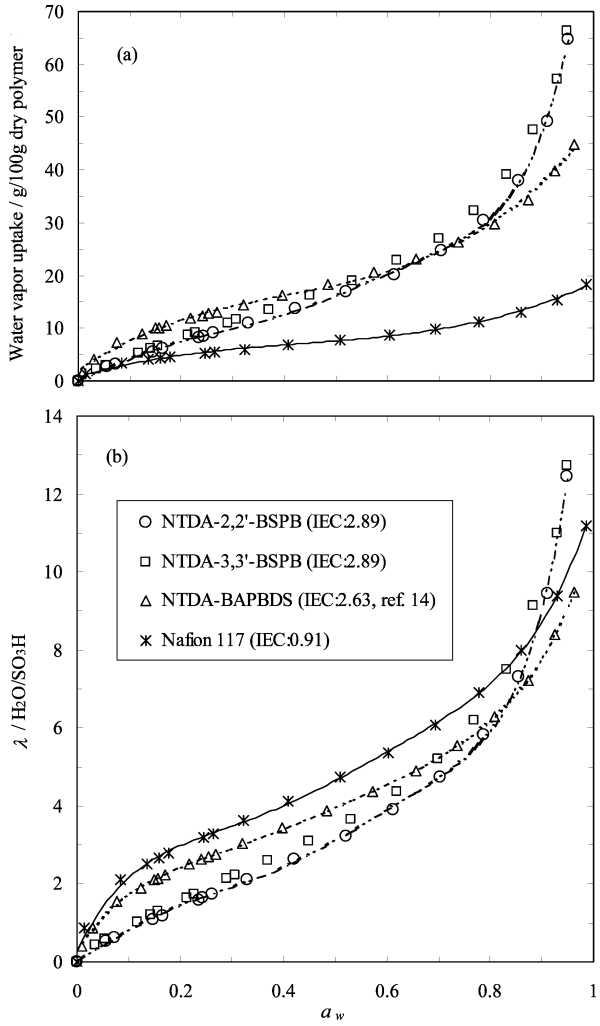

Fig. 4 Water vapor sorption isotherms of sulfonated polymer membranes at 323 K.

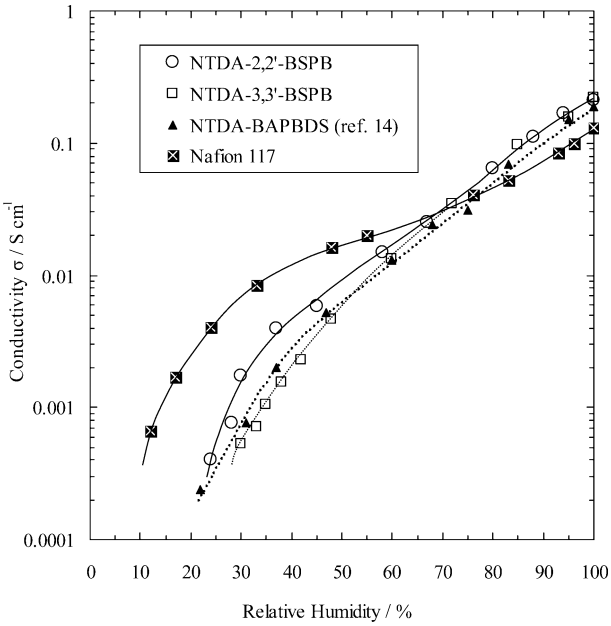

Fig. 5 Proton conductivity of SPI membranes as a function of relative humidity at 323 K (The values at 100% RH refer to those measured in liquid water).

Proton conductivity

Fig. 5 shows the proton conductivities of SPIs and Nafion 117 membranes as a function of RH at 323 K. The σ-RH

relationship of the BSPB-based SPIs was similar to that of the main-chain-type SPI with the similar IEC, NTDA-BAPBDS, but slightly different from that of Nafion 117. With an increase in RH, the proton conductivity increased more largely for the SPIs than for Nafion 117. In the range of RH above 80%, the proton conductivities were higher for the SPIs than for Nafion 117. The σ values of the SPIs in water were around 0.20 S cm^{-1}, which were about 2 times larger than that of Nafion117.

Based on the water uptake and density of dry membrane (ρ_P) under the assumption of the additive law of volume of water and polymer, the water volume fraction, C, was calculated from eqn. (4):

$$C = \frac{V_{water}}{V_{total}} = \frac{V_{water}}{V_{water} + V_{dry}} = \frac{WU}{WU + 100/\rho_P} \quad (4)$$

The ρ_P values of SPIs were evaluated as 1.61, 1.57 and 1.55 g cm^{-3} for NTDA-2,2′-BSPB, NTDA-3,3′-BSPB and NTDA-BAPBDS, respectively, from the density values at 70% RH listed later in Table 5. The ρ_P value of 2.3 g cm^{-3} was used for Nafion 117.[27] The σ data in Fig. 5 were replotted in the form of log σ *vs.* log C in Fig. 6. The SPIs and Nafion 117 membranes displayed the similar σ-C relationship that with increasing C, the σ increased first sharply, then slowly and finally leveled off. It is suggested that the proton conduction paths are developed well enough to give high proton conductivities for these membranes equilibrated at high RHs above 90% ($C > 0.3$). Compared with Nafion 117, the higher conductivities of the SPIs in a fully hydrated state are due to their higher IECs. On the other hand, in the range of lower C, Nafion membrane showed much higher proton conductivities than the SPIs. This is because Nafion membrane possesses high ion density clusters that have been proposed to form ion-rich channels being favorable for proton transport.[28] The SPIs especially NTDA-BAPBDS needed much larger C values to display the same proton conductivity as that of Nafion. This suggests the presence of a threshold water volume fraction C_0, below which proton conduction is impossible, and the different threshold values for these membranes.

The proton conductivity in some proton-conducting polymer membranes has been reported to obey the following percolation theory as shown in eqn. (5).[27,29,30]

$$\sigma = \sigma_0(C - C_0)^n \quad (5)$$

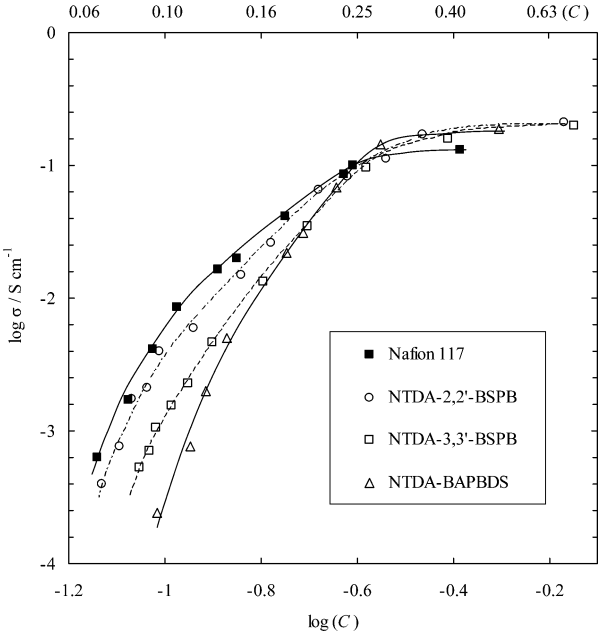

Fig. 6 Proton conductivity of SPI membranes and Nafion 117 as a function of water volume fraction at 323 K.

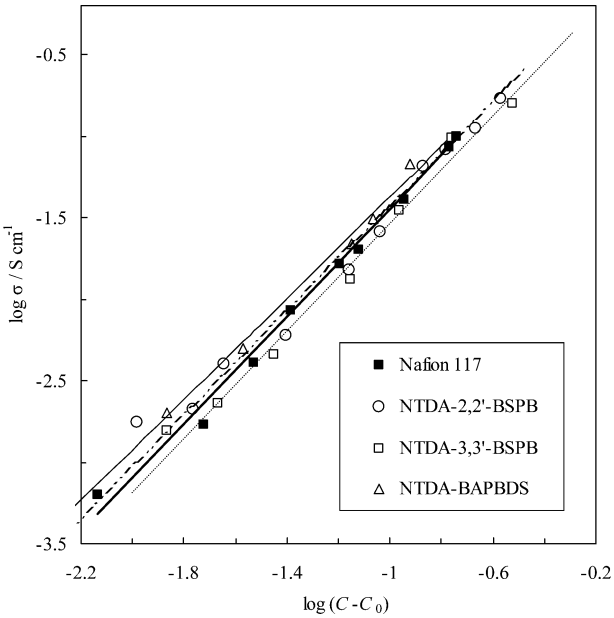

Fig. 7 Data and best-fit lines for conductivity *vs.* water volume fraction minus percolation threshold for SPIs and Nafion 117 at 323 K.

where C_0 is a threshold volume fraction required for protons to transport, n is referred to as a critical exponent that controls the scaling behavior, and σ_0 is a prefactor determined by carrier number and ion transport mobility.

To test the percolation theory, C_0 was initially chosen as a minimum C value for each membrane in Fig. 6 and the calculated line of log σ vs. log (C–C_0) was best fit to the experimental data except for the datum measured in water. This procedure was repeated for various values of C_0 until a maximum fitting of the calculated and the experimental data was achieved. The experimental data and best-fit line for SPI membranes and Nafion 117 are shown in Fig. 7. The best-fit parameters are listed in Table 2. For a three dimensional continuous random system, C_0 has been reported to be 0.15 and n has been reported to range between 1.3 and 1.7.[27,29,30] The percolation thresholds of the SPIs and Nafion117 were in the range of 0.065 to 0.105, and less than 0.15. The probable explanation is that a smaller threshold volume fraction would be expected if ion clusters and therefore water molecules are spread into a more extended network.[27,29,30] As mentioned above, the side-chain-type SPIs, NTDA-BSPB, have microphase-separated structure where the ionic domains connected to each other to form proton-conducting pathways. This is likely the reason for the lower C_0 for NTDA-BSPB.

Fig. 8 shows the temperature dependence of proton conductivity for NTDA-BSPB membranes and Nafion 117 in liquid water and for NTDA-2,2′-BSPB membrane at 80%RH. The activation energies ΔE_a of proton conductivity in water were 11 KJ mol^{-1} for NTDA-BSPB and 12 KJ mol^{-1} for Nafion 117, which were similar to the reported values for Nafion 117 (ΔE_a = 9–13 KJ mol^{-1}) and sulfonated polysulfone (ΔE_a = 10–12 KJ mol^{-1}).[31] The ΔE_a at 80% RH

Table 2 Percolation fit parameters

Sulfonated Polymer	C_0	n	σ_0/S cm^{-1}
NTDA-2,2′-BSPB	0.075	1.60	1.50
NTDA-3,3′-BSPB	0.090	1.65	1.40
NTDA-BAPBDS	0.105	1.55	1.50
Nafion 117	0.065	1.65	1.50

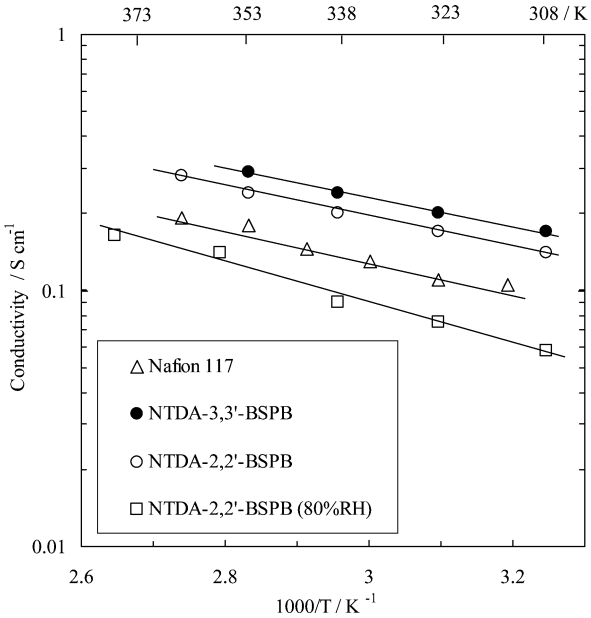

Fig. 8 Temperature dependence of proton conductivity for SPIs and Nafion 117 in liquid water or at 80% RH.

was 15 KJ mol^{-1} for NTDA-2,2′-BSPB, which was a little larger than that in water. This SPI displayed high proton conductivities of 0.14–0.16 S cm^{-1} at temperatures higher than 353 K at 80% RH, which is promising for PEFC applications at medium temperatures.

Table 3 shows comparison of the water uptakes and proton conductivities among typical side-chain-type sulfonated polymers. It should be mentioned that the proton conductivities of NTDA-2,2′-BSPB and NTDA-3,3′-BSPB were comparable to or higher than those of the sulfonated polymers reported in the literature.[17–22,32] For example, Roziere and co-workers[19] reported a proton conductivity of 0.017 S cm^{-1} for benzylsulfonate grafted polybenzimidazole (PBI-BzS, sulfonation degree of 85 mol%) at 313 K and 100% RH, which was much lower than those of the SPIs. Rikukawa and co-workers reported a little higher proton conductivities of 0.17 and 0.19 S cm^{-1} for PBI-BS and S-PPBP, although their water uptakes were not reported.[17,22] Holdcroft *et al.*[32] recently synthesized a series of graft polymers comprising graft chains of macromonomer poly (styrenesulfonic acid) (macPSSA) and a polystyrene (PS) backbone. In spite of the relatively low water uptakes, they displayed high proton conductivities of 0.05–0.24 S cm^{-1} because of a higher degree of phase separation of ionic domains. On the other hand, BSPB-based SPIs displayed higher σ values than NTDA-DAPPS under the same conditions, due to their slightly higher *WU*s resulting from the larger IECs, and better microphase separation.

Membrane stability

For a polymer electrolyte membrane, it is important not only to have high proton conductivity but also to have properties making it amenable to membrane-assembly formation, including good water stability, better dimensional stability, appropriate mechanical property, and reasonable thermal stability. The water stability of SPI membranes is summarized in Table 4. The stability test of SPI membranes toward water was carried out by immersing the membranes into water at a given temperature (353 or 373 K) and is justified by the loss of mechanical strength of the hydrated membranes. The criterion for the judgment of the loss of mechanical strength is that the membrane is broken after being lightly bent at 353 K in water, or starts to be broken into pieces under boiling (373 K).

We have previously reported that the water stability of SPI membranes is influenced by IEC, *WU*, flexibility of the polymer chain, and basicity of the sulfonated diamines.[12–14] Membranes with high IECs tend to yield large *WU*s and thus poor water stability, and *vice versa*. Polyimides with flexible structure and high basicity of the sulfonated diamine moieties tend to have good water stability because the flexibility allows easy relaxation of polymer chain and the high basicity of the sulfonated diamine moieties depresses the hydrolysis of imido rings. This is why the water stability is in the following order for main-chain-type SPI membranes including different diamine moieties: BAPBDS ≫ ODADS, BAPFDS ≫ BDSA.[12–14] As shown in Table 4, NTDA-2,2′-BSPB and NTDA-3,3′-BSPB displayed much better water stability than the main-chain-type SPIs despite their high IEC and high *WU*s. The membranes could bear the immersion in boiling water (373 K) up to 700 h for NTDA-3,3′-BSPB and 2500 h for NTDA-2,2′-BSPB. The excellent water stability of NTDA-BSPB membranes may partly come from the higher basicity of the diamine moieties. BSPB is more basic than ODADS because of the strong electron donating effect of the propoxy groups. Furthermore, the flexible sulfopropoxy groups are favorable to aggregate into hydrophilic domains and the polyimide backbones form hydrophobic domains. Because the hydrolysis of the imido ring is an acid-catalytic reaction, if the protons are mostly restricted in the ion-rich domains isolated from the polymer main chain, the hydrolysis of the imido ring of the SPI will be depressed. This is another likely reason for the excellent water stability of NTDA-BSPB. NTDA-3,3′-BSPB displayed poorer water stability than NTDA-2,2′-BSPB although the diamines are very structurally similar (isomers to each other). The results suggest that the substitution position of the sulfonic acid groups had significant influence on the membrane stability. The longer the distance between the sulfonic acid group and the amine group, the better the water stability of the resulting SPI. The meta-sulfopropoxylated polyimide was more stable than the *ortho*-sulfopropoxylated one.

It is interesting that the BSPB isomer-based SPI membranes also showed much better water stability than another

Table 3 Water uptake and proton conductivity of side-chain-type sulfonated polymer membranes

Membranes	IEC[a]/meq. g^{-1}	T/K	RH (%)	*WU*/g/100 g dry polymer	σ/S cm^{-1}	Ref.
NTDA-2,2′-BSPB	2.89 (2.72)	323	90	47	0.12	This paper
NTDA-3,3′-BSPB	2.89 (2.80)	323	90	50	0.11	This paper
NTDA-DAPPS	2.09 (1.98)	323	90	40	0.035	25
PBI-BS	—	333	100	—	0.003	17
PBI-BS	—	323	90	—	0.17	18
S-PPBP	1.85	323	100	29[b]	0.01	22
S-PPBP	2.61	323	90	—	0.19	23
PBI-BzS	1.57	313	100	33[b]	0.017	19
PS-g-macPSSA	1.35	rt	In water	37	0.054	32
PS-g-macPSSA	1.56	rt	In water	48	0.24	32
Nafion 117	0.91	323	90	14	0.085	This paper

[a] The data in parenthesis are experimental values and others are calculated values. [b] Measured at room temperature.

Table 4 IEC, water uptake and water stability of SPI membranes

Polyimide	IEC[a]/meq g^{-1}	WU^b	Water stability[c] T/K	Time/h	Ref.
NTDA-2,2′-BSPB	2.89(2.72)	222	353	>4000	This paper
			373	2500	This paper
NTDA-3,3′-BSPB	2.89(2.80)	250	353	1000	This paper
			373	700	This paper
NTDA-ODADS/ODA(3/1)	2.70(2.31)	113	353	10	12
NTDA-BAPBDS	2.63(2.58)	103	373	1000	14
NTDA-DAPPS	2.09(1.98)	105	353	200	25

[a] The data in parenthesis are measured values, others are calculated ones. [b] Measured at 323 K, *WU*: g per 100 g dry polymer. [c] Elapsed time when the samples began to loose mechanical strength.

Table 5 Density and dimensional change of SPI membranes at 293 K

SPIs	Density[a]/g cm^{-3} 70% RH	In water	WU^b	Δt_c	Δl_c	Ref.
NTDA-2,2′-BSPB	1.438	1.142	210	2.3	0.01	This paper
NTDA-3,3′-BSPB	1.402	1.130	220	1.8	0.11	This paper
NTDA-DAPPS	1.452	1.305	91	0.12	0.15	25
NTDA-BAPBDS	1.399	1.274	75	0.16	0.15	14

[a] Measured for samples equilibrated at 70% RH or in water, respectively. [b] Measured for samples after being immersed in water for 5 h.

Table 6 Results of Fenton's reagent (30 ppm $FeSO_4$ in 30% H_2O_2) test of SPI membranes at 298 K

Membranes	IEC/ meq g^{-1}	Thickness/ μm	$\tau_1{}^a$	$\tau_2{}^a$	Ref.
NTDA-2,2′-BSPB	2.89	16	18	22	This paper
NTDA-3,3′-BSPB	2.89	22	13	16	This paper
NTDA-ODADS–ODA (1 : 1)	1.95	29	24	—	12
NTDA-BAPBDS	2.63	35	22	25	14

[a] τ_1 and τ_2 refer to the elapsed time (h) when the membranes began to dissolve and when they had dissolved completely.

side-chain-type SPI membrane, NTDA-DAPPS, with the same side group. This is likely because DAPPS is a *meta*-oriented (nonlinear configuration) diamine, whereas BSPB isomers are *para*-oriented ones (linear configurations). The polyimides derived from *meta*-oriented diamines generally have better solubility than those from *para*-oriented ones. Actually, NTDA-DAPPS showed better solubility properties than NTDA-BSPB, which is responsible for its poor water durability. In addition, the DAPPS-derived SPI was not favorable to have clear microphase separation due to its structure and low IEC.

Table 5 lists the density and dimensional changes of SPI membranes at room temperature (293 K). The dimensional changes (Δt_c and Δl_c) were calculated using the dimensions at 70% RH as the standards. NTDA-2,2′-BSPB and NTDA-3,3′-BSPB membranes displayed very large *WU*s in liquid water resulting in very large size changes. Although the size change in diameter was negligibly small, the change in thickness was rather large, indicating a clear anisotropy in membrane swelling for the BSPB-based SPIs. This behavior is quite different from that of the main-chain-type SPI such as NTDA-BAPBDS and another side-chain-type SPI, NTDA-DAPPS, where the membrane swelling was rather isotropic.

In order to check the hydrolysis stability of sulfopropoxy groups of the side-chain-type SPI membranes, aging experiments were carried out. The SPI membranes were immersed in 0.1 M sulfuric acid at 373 K for 300 h, and the IEC and proton conductivity were measured before and after the treatment. It was found that the IEC of NTDA-3,3′-BSPB was unchanged (2.80 meq g^{-1}) after the membrane was treated in boiling aqueous acid for 300 h. The proton conductivity of NTDA-2,2′-BSPB membrane also remained unchanged (around 0.24 S cm^{-1} at 353 K in liquid water) after treatment under the same conditions. These results indicate that the hydrolysis of sulfopropoxy groups did not occur under the present conditions.

The oxidative stability of SPI membranes was also investigated by immersing the samples (the size of each sheet: 1.0 × 1.0 cm^2) into Fenton's reagent (30 ppm $FeSO_4$ in 30% H_2O_2) at 298 K. The oxidative stability was characterized by the time that had elapsed when the membranes started to dissolve and when they had dissolved completely. As shown in Table 6, NTDA-2,2′-BSPB membrane displayed the oxidative stability similar to that of the main-chain-type SPIs, whereas NTDA-3,3′-BSPB displayed a little lower oxidative stability.

Conclusions

(1) Two kinds of sulfonated diamine isomers bearing sulfopropoxy groups (2,2′-BSPB and 3,3′-BSPB) were successfully synthesized. The highly sulfonated polyimides with sulfonic acid groups in the side chains were prepared from these diamines and NTDA. (2) BSPB-based SPIs had a microphase-separated structure composed of hydrophilic ionic domains and hydrophobic polyimide domains. (3) These SPIs showed lower proton conductivities than Nafion 117 at RHs below 60%, but higher conductivities at RHs above 70%. The proton conducting behavior could be explained by percolation theory. The percolation thresholds of NTDA-2,2′-BSPB and NTDA-3,3′-BSPB were 0.075and 0.090, respectively, which were higher than that of Nafion 117 (C_0 = 0.065) and lower than that of a main-chain-type SPI, NTDA-BAPBDS (C_0 = 0.105). (4) BSPB-based SPIs showed excellent water stability compared with the main-chain-type ones, due to the microphase-separated structure and the higher basicity of BSPB diamines. The meta-sulfopropoxylation (2,2′-BSPB) led to much better water stability of the resulting SPI than the *ortho*-sulfopropoxylation (3,3′-BSPB). The sulfopropoxy groups were stable in aqueous acidic solution at 373 K for more than 300 h. (5) BSPB based SPIs displayed clear anisotropy in membrane swelling and the dimensional change in thickness was much larger than that in plane direction.

Acknowledgements

This work was supported partly by a Grant-in-aid for Exploratory Research (No. 14655294) from the Ministry of Education, Culture, Sports, Science and Technology of Japan.

References

1 P. Costamagna and S. Srinivasan, *J. Power Sources*, 2001, **102**, 242.
2 P. Costamagna and S. Srinivasan, *J. Power Sources*, 2001, **102**, 253.

3 J. A. Kerres, *J. Membr. Sci.*, 2001, **185**, 3.
4 S. D. Mikhailenko, S. M. J. Zaidi and S. Kaliaguine, *J. Polym. Sci.: Part B: Polym. Phys.*, 2000, **38**, 1386.
5 H. R. Allcock, M. A. Hofmann, C. M. Ambler, S. N. Lvov, X. Y. Zhou, E. Chalkova and J. Weston, *J. Membr. Sci.*, 2002, **201**, 47.
6 S. Faure, R. Mercier, P. Aldebert, M. Pineri and B. Sillion, *French Pat.*, 9605707/1996.
7 S. Faure, N. Cornet, G. Gebel, R. Mercier, M. Pineri and B. Sillion, *Proceedings of Second International Symposium on New Materials for Fuel Cell and Modern Battery Systems*, eds. Ecole Polytechnique de Montreal, Montrtreal, Canada, July 6–10, 1997, P818.
8 E. Vallejo, G. Porucelly, C. Gavach, R. Mercier and M. Pineri, *J. Membr. Sci.*, 1999, **160**, 127.
9 C. Genies, R. Mercier, B. Sillion, N. Cornet, G. Gebel and M. Pineri, *Polymer*, 2001, **42**, 359.
10 Y. Zhang, M. Litt, R. F. Savinell, J. S. Wainright and J. Vendramini, *Polymer Prepr. (Am. Chem. Soc., Div. Polym. Chem.)*, 2000, **41**, 1561.
11 H. J. Kim and M. Litt, *Polymer Prepr. (Am. Chem. Soc., Div. Polym. Chem.)*, 2001, **42**, 486.
12 J. Fang, X. Guo, S. Harada, T. Watari, K. Tanaka, H. Kita and K. Okamoto, *Macromolecules*, 2002, **35**, 9022.
13 X. Guo, J. Fang, T. Watari, K. Tanaka, H. Kita and K. Okamoto, *Macromolecules*, 2002, **35**, 6707.
14 T. Watari, J. Fang, K. Tanaka, H. Kita, K. Okamoto and T. Hirano, *J. Membr. Sci.*, 2004, **230**, 111.
15 M. B. Gieselman and J. R. Reynolds, *Macromolecules*, 1992, **25**, 4832.
16 M. B. Gieselman and J. R. Reynolds, *Macromolecules*, 1993, **26**, 5633.
17 J. M. Bae, I. Honma, M. Murata, T. Yamamoto, M. Rikukawa and N. Ogata, *Solid State Ionics*, 2002, **147**, 189.
18 H. Manabe, M. Kawahara, M. Rikukawa and K. Sanui, *Polymer Preprints, Japan*, 2000, **49**, 3215.
19 X. Glipa, M. E. Haddad, D. J. Jones and J. Roziere, *Solid State Ionics*, 1997, **97**, 323.
20 K. Miyatake and A. S. Hay, *J. Polym. Sci., Part A: Polym. Chem.*, 2001, **39**, 3211.
21 K. Miyatake, K. Oyaizu, E. Tsuchida and A. S. Hay, *Macromolecules*, 2001, **34**, 2065.
22 T. Kobayashi, M. Rikukawa, K. Sanui and N. Ogata, *Solid State Ionics*, 1998, **106**, 219.
23 T. Yamamoto, M. Rikukawa and K. Sanui, *Polymer Preprints, Japan*, 2000, **49**, 3503.
24 *Polyimides: Fundamentals and Applications (Marcel Dekker: New York,* eds. M. K. Ghosh and K. L. Mittal, 1996, p7.
25 Y. Yin, J. Fang, Y. Cui, K. Tanaka, H. Kita and K. Okamoto, *Polymer*, 2003, **44**, 4509.
26 T. Watari, H. Wang, K. Kuwahara, K. Tanaka, H. Kita and K. Okamoto, *J. Membr. Sci.*, 2003, **219**, 137.
27 C. A. Edmondson and J. J. Fontanella, *Solid State Ionics*, 2002, **152–153**, 355.
28 T. D. Gier, G. E. Munn and F. C. Wilson, *J. Polym. Sci., Polym. Phys. Ed.*, 1981, **19**, 1687.
29 W. Y. Hsu, J. R. Barkley and P. Meakin, *Macromolecules*, 1980, **13**, 198.
30 T. Xu, W. Yang and B. He, *Chem. Eng. Sci.*, 2001, **56**, 5343.
31 F. Lufrano, I. Gatto, P. Staiti, V. Antonucci and E. Passalacqua, *Solid State Ionics*, 2001, **145**, 47.
32 J. Ding, C. Chuy and S. Holdcroft, *Macromolecules*, 2002, **35**, 1348.